Sensors and Materials, Vol. 11, No. 3 (1999) 149–162
MYU Tokyo

S & M 0362

Problems in Gas Sensor Measuring Circuit and Proposal of New Circuit

Arporn Teeramongkonrasmee and Mana Sriyudthsak

Department of Electrical Engineering, Faculty of Engineering, Chulalongkorn University, Phaya-Thai Rd., Patumwan, Bangkok 10330, Thailand

(Received March 28, 1998; accepted December 11, 1998)

Key words: gas sensors, measuring circuit, sensitivity, recovery time, series resistance

An analysis including the nonlinear characteristic of gas sensors shows that the conventional gas measuring circuit is not suitable for determining gas sensitivity ($S = R_{air}/R_{gas}$). This circuit exhibits a dependence of sensitivity on the values of external circuit components, i.e., series resistance (R) and voltage source (V_{in}). Moreover, the dynamic parameters, such as recovery time, are also strongly affected by these external components. These problems prevent the use of the conventional circuit in the comparison of gas sensing performance and gas sensitivity among different sensors. A novel gas measuring circuit is proposed to overcome these problems. In this new circuit, the electrical operating point of the semiconductor gas sensor is kept at a constant value and is not disturbed by the change of the external resistance. The experimental results showed that the new circuit gave a nearly constant sensitivity and faster recovery time.

1. Introduction

Semiconductor gas sensors are widely used to detect inflammable and toxic gases in domestic and industrial environments because of their low cost and simplicity. The operation of gas sensors is based on the change of electrical conductance caused by gas absorption.[1,2] In general, the sensing performance of gas sensors is indexed by the sensor sensitivity (S) which is defined as the ratio of the sensor resistance in air (R_{air}) to the resistance in gas ambient (R_{gas}), as shown in eq. (1).

$$S = \frac{R_{air}}{R_{gas}} \tag{1}$$

Thus, a circuit for calculating sensor resistance is needed. The conventional circuit for determining the sensor resistance, a simple voltage divider, is shown in Fig. 1. This circuit is widely used because of its simplicity in practical uses. This conventional circuit can determine the sensor resistance correctly if the gas sensor acts as a linear resistive element. Unfortunately, a real gas sensor is much more complex, since the potential barriers at the grain boundaries cause this device to have a nonlinear current-voltage (I-V) characteristic. The external circuit components such as resistance (R) and voltage source (V_{in}), therefore, affect the calculation of sensitivity as well as gas sensitivity. This critical situation makes the comparison of the sensitivity among different sensors impossible. Even though the same gas sensor is characterized, a different value of sensitivity may be obtained if different values of R and V_{in} are chosen. Moreover, the electrical operating point established between the gas sensor and the external circuit components also controls the dynamic characteristics of the gas sensor. Since the capacitance (C) at the grain boundary also exhibits a voltage-dependent characteristic, it can be observed by monitoring the change of the recovery time of the gas sensor with R or V_{in}. To overcome these problems, a thorough understanding of the interaction between the gas sensor characteristics and the gas measuring circuit is necessary.

The aim of this work is to clarify the effects of the external components, such as resistance, in the conventional measuring circuit on gas sensing parameters. The parameters of interest are sensitivity and recovery time. A novel measuring circuit with a fixed bias voltage is proposed to solve these problems. SnO_2 thick film gas sensors and a flow injection analysis were used in the experiments.

2. Analysis of Measuring Circuit

2.1 *Conventional circuit*

Figure 1(a) shows the schematic diagram of the conventional circuit. The I-V characteristic and the load line for this circuit are also depicted in Fig. 1(b). Normally, the sensor resistance (R_s) is calculated from the output voltage (V_{out}),

$$R_s = R \cdot \left(\frac{V_{in}}{V_{out}} - 1 \right), \tag{2}$$

where R and V_{in} are the external resistance and the voltage source, respectively. However, this equation does not show explicitly how R_s is dependent on R. In order to demonstrate the effect of the external components, here we adopted the load line concept[3,4] to gain insight into the operation of the gas sensor in this circuit. The concept of the load line can be applicable to a device having either a linear or a nonlinear I-V characteristic. The load line equation for this circuit can be given as

$$I = \frac{V_{in}}{R} - \frac{V_s}{R}, \tag{3}$$

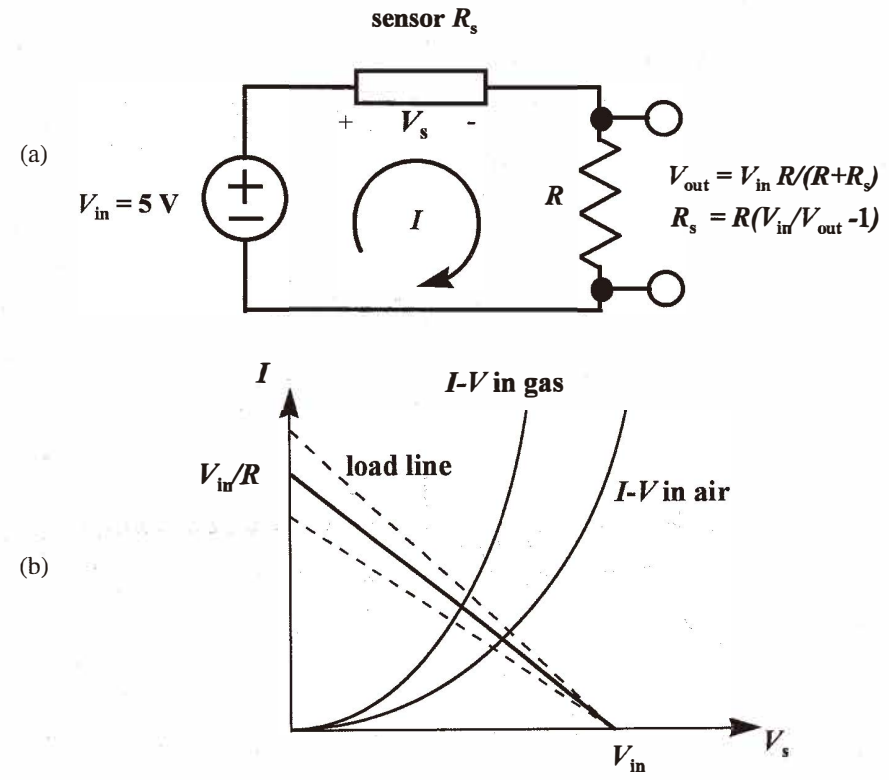

Fig. 1. (a) Schematic diagram of the conventional measuring circuit using a voltage divider and (b) gas sensor characteristics and the load line for the circuit.

where I is the current flow through the gas sensor. Equation (3) describes a straight line, called the load line (Fig. 1(b)). Note that the slope and intercept of the load line depend only on R and V_{in}. It is known that I-V relations of a gas sensor or other sintered ceramic devices may be described by the empirical equation[5]

$$I = C V^{\alpha}, \tag{4}$$

where C is the proportional constant and α is the nonlinear coefficient. It should be noted that if $\alpha = 1$, the gas sensor will have a linear I-V characteristic.

Both eqs. (3) and (4) must be satisfied simultaneously. The point at their intersection is called the quiescent or operating point. It is instructive to investigate the changes that occur in the operating point for the conventional circuit as V_{in} and R vary. These changes are depicted in Figs. 2(a) – (d).

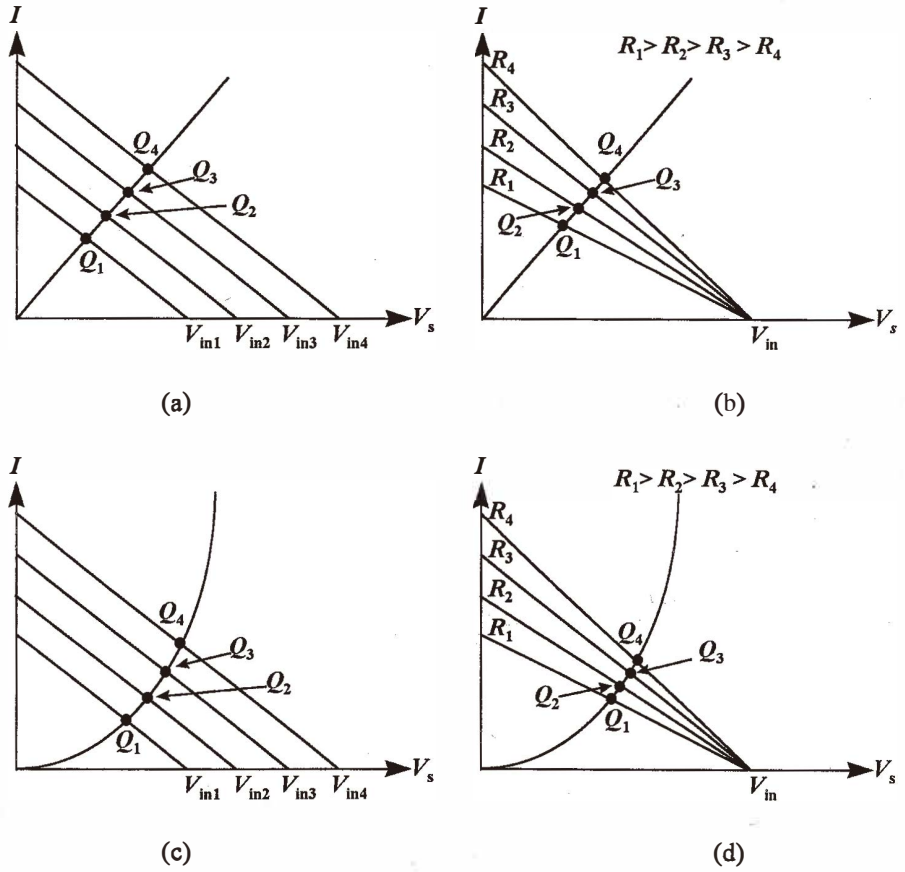

Fig. 2. Changes in operating point in the conventional circuit in the case of a linear *I-V* characteristic of gas sensor where (a) V_{in} and (b) R vary, and the case of a nonlinear *I-V* characteristic where (c) V_{in} and (d) R vary.

It is clear that for the linear case ($\alpha = 1$), no matter how R and V_{in} are varied or the operating point is changed, the resistance of the gas sensor (1/slope at Q points that is V/I) remains constant. For the nonlinear case ($\alpha \neq 1$), as R or V_{in} changes, sensor resistance is shifted to a new value. This results in the dependence of gas sensitivity on R and V_{in}. Thus, different bias conditions will lead to different values of S, and the comparison of gas sensing performance among various sensors becomes impossible. Moreover, even if the same gas sensor is used, different values of S will be obtained if it is characterized under different bias conditions (Fig. 7(a)).

By using eq. (4), we can derive the following expression of S for this circuit.

$$S = \frac{C_{\text{gas}}}{C_{\text{air}}} \left(\frac{V_{\text{s in gas}}^{\alpha_{\text{gas}}-1}}{V_{\text{s in air}}^{\alpha_{\text{air}}-1}} \right) \tag{5}$$

Here, the subscripts indicate whether the condition of the parameters is in air or in gas ambient. The voltage across the gas sensor can be obtained by solving eqs. (2) and (3). In the special case (the linear I-V characteristic), α_{air} and $\alpha_{\text{gas}} = 1$, hence eq. (4) can be reduced to the simplest form.

$$S = \frac{C_{\text{gas}}}{C_{\text{air}}}; \ \alpha_{\text{gas}} \text{ and } \alpha_{\text{air}} = 1 \tag{6}$$

It is clear that in this case, S is constant, and C_{air} and C_{gas} are equivalent to the conductance of the gas sensor in air and in gas ambient, respectively.

2.2 *Novel measuring circuit*

To eliminate the problem in which S and R_s change with both R and V_{in} in the conventional circuit, an alternative circuit was designed to keep the operating point of the gas sensor independent of R. The schematic diagram of the proposed circuit is shown in Fig. 3(a), and the load line of the proposed circuit is represented by the vertical line in Fig. 3(b). Any change in R has no effect in the calculation of sensor resistance. The vertical load line means that the operating point is controlled only by the external voltage source. In other words, the voltage across the gas sensor is always constant ($V_s = V_{\text{in}}$). The current through the gas sensor is converted to the voltage signal via an Op-Amp and an external resistance. The relation between R_s and V_{out} can be given as follows.

$$R_s = \frac{V_{\text{in}}}{V_{\text{out}}} R \tag{7}$$

One can easily show that the gas sensitivity can be obtained directly from the ratio expressed by eq. (7).

$$S = \frac{R_{\text{air}}}{R_{\text{gas}}} = \frac{V_{\text{out in gas}}}{V_{\text{out in air}}} \tag{8}$$

By applying the I-V relation in eq. (3), we can express S as a function of C and α.

$$S = \frac{C_{\text{gas}}}{C_{\text{air}}} V_{\text{in}}^{(\alpha_{\text{gas}}-\alpha_{\text{air}})} \tag{9}$$

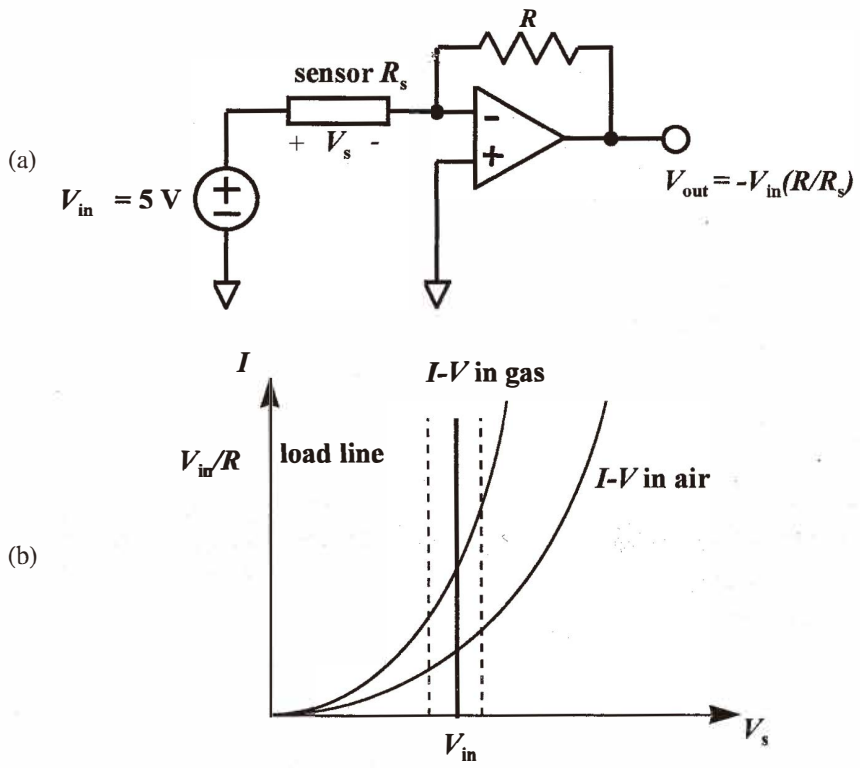

Fig. 3. (a) Schematic diagram of proposed measuring circuit and (b) gas sensor characteristic and load line for this circuit.

This equation clearly shows that gas sensitivity depends only on one external component, i.e., V_{in}. Therefore, if we keep V_{in} the same for all gas sensors, gas sensitivities from different sensors can be compared.

3. Experiments

SnO_2 powder was prepared from $SnCl_4$ by the coprecipitation technique.[6,7] $SnCl_4$ aqueous solution was neutralized by ammonia solution (30%), which resulted in the precipitation of stannic acid. Then, the precipitated powder was washed thoroughly with de-ionized (DI) water to remove NH_4^+ and Cl^- ions. This powder was calcined at 80°C for 24 h, followed by sintering at temperatures of 300, 400, 500 or 600°C for 3 h. The average size of SnO_2 crystallite was calculated from the specific surface areas determined by the

BET method. The SnO_2 grain size was distributed in the range of 5–38 nm according to the sintering temperature as shown in Fig. 4.

SnO_2 thick film gas sensors were fabricated on glass substrates having two Ti/Pt electrodes. The space between electrodes was 1 mm. Figure 5 shows the structure of the fabricated sensors. They were installed in a flow injection system. The details of the experimental setup have been described elsewhere.[8] Synthetic air containing 20% oxygen and 80% nitrogen was used as a carrier gas. The total flow rate was set at 400 ml/min. The temperature of gas sensors was fixed at 300°C, and 0.1% alcohol solution was used throughout the experiments.

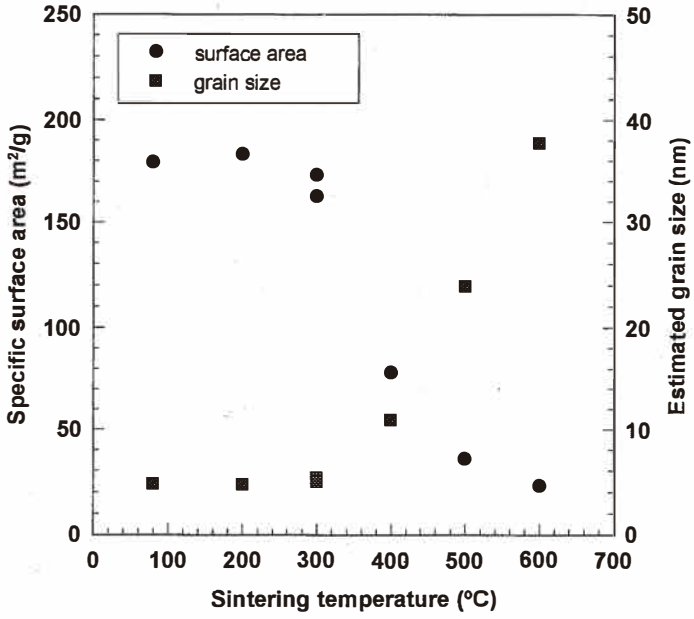

Fig. 4. Specific surface area and average grain size of SnO_2 as a function of sintering temperatures.

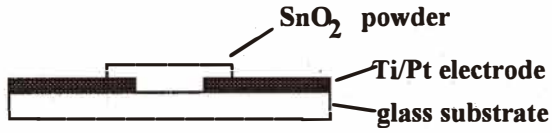

Fig. 5. Structure of gas sensors.

4. Results and Discussions

Figure 6 shows the typical response curves of a gas sensor obtained using the conventional measuring circuit and our proposed circuit. The abrupt changes in the voltage of the signal represented the points at which gas samples were injected into the gas measuring system. As can be seen in Fig. 6, the whole system exhibited quite stable signals and excellent repeatability.

(a)

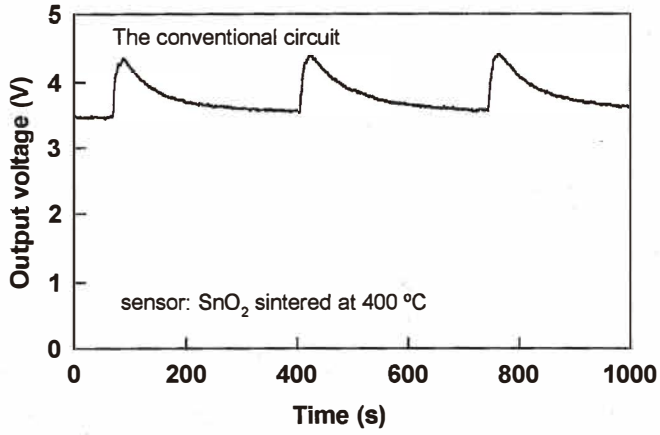

(b)

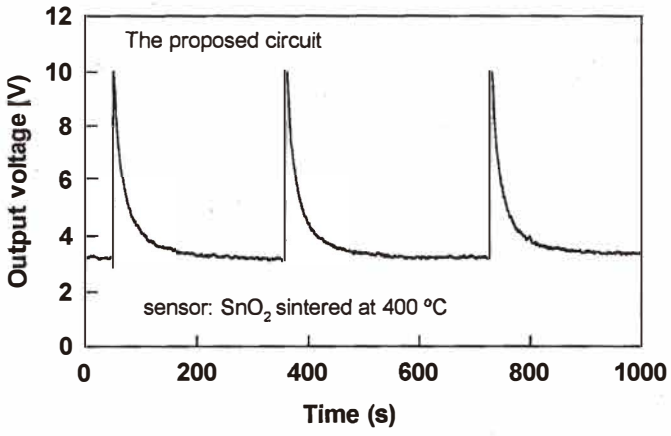

Fig. 6. Response curves obtained from (a) the conventional circuit and (b) the proposed circuit.

4.1 *Effect of external resistance on gas sensitivity*

Two sets of experiments were conducted to verify the analytical results of the conventional circuit and the proposed circuit. SnO_2 sensors sintered at 300, 400, 500 and 600°C were used. The value of the external resistance was varied from 1 kΩ to 10 MΩ. In all experiments, the voltage source was set to 5 V. Figure 7 shows the variation of gas sensitivity with the external resistance in both circuits. According to the data, we could classify gas sensors into two main groups. The first group consisted of SnO_2 gas sensors sintered at 300 and 400°C. The other group consisted of the sensors sintered at 500 and 600°C. In the former group, gas sensitivity was nearly constant with respect to the variation of R. In the latter group, gas sensitivity increased montonically as R decreased. It can be observed in Fig. 7(a) that in the conventional circuit, the calculated sensitivities may have values differing up to five or six fold. This difference made the conventional circuit unsuitable for comparing the gas sensing performance.

It is well known that the conductivity of a SnO_2 sensor is predominantly determined by contributions of nanocrystals. By considering the mean grain size of the SnO_2 powders, we may, therefore, be able to determine why the SnO_2 sensors exhibited two different characteristics as shown in Fig. 7(a). The results of the BET analysis indicated that the 300 and 400°C-sintered SnO_2 sensors consisted of ultrafine grains with the grain sizes D of about 5 and 10 nm, respectively. Here, it should be noted that the Debye length, L_D of SnO_2 material in air is about 3 nm.[9] Hence, the grain size of these sensors was comparable with or less than $2L_D$. This implied that the whole grains of the SnO_2 powder were covered with the depletion region or the transducer function was operated by the grain control mechanism,[10] whereas the 500 and 600°C-sintered SnO_2 sensors had the grain sizes of 23 and 38 nm, respectively, which are greater than $2L_D$. This means that the conduction mechanism was mainly controlled by the potential barrier at the grain boundary. Thus, the transducer function of these sensors should be governed by the grain boundary control.

The solid lines in Fig. 7(a) represent the fitted results obtained using eqs.(4) – (6) and the values in Table 1. The values of C and α for SnO_2 gas sensors are summarized in Table 1. These values were calculated from I-V characteristics; examples of I-V curves are given in Fig. 8. The results fit quite well with the experimental data in Fig. 7(a). It should be noted that α of all sensors was greater than 1. This implies that all the sensors possess the nonlinear I-V characteristic. Moreover, it is clear that the dependence of S on R is determined mainly by α.

In the proposed circuit, S of all sensors was nearly constant independent of the external resistive component. These results are shown in Fig. 7(b). However, the 300°C-sintered SnO_2 sensor showed a decrease of S at very low values of R. The solid line in Fig 7(b) is calculated using eq. (9) and the values in Table 1. Although, the experimental data from 500 and 600°C-sintered SnO_2 gas sensors exhibited some differences from the calculated results, they show the trend predicted by eq. (9). The α values in Table 1 were the average values in the range of 0 – 5 V. However, in the much more complex model, α is also a function of current. As can be seen in Fig. 7(a), the theoretical values worked quite well at the moderate to high values of R, and started to deviate from the experimental results at the very small values of R. The discrepancy between the experimental results and the theoretical results may occur from the assumption of the constant α in eq. (4).

(a)

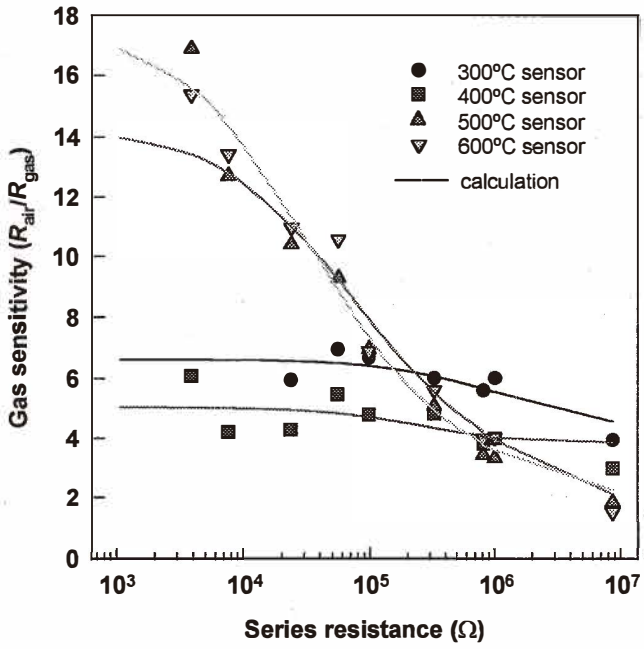

(b)

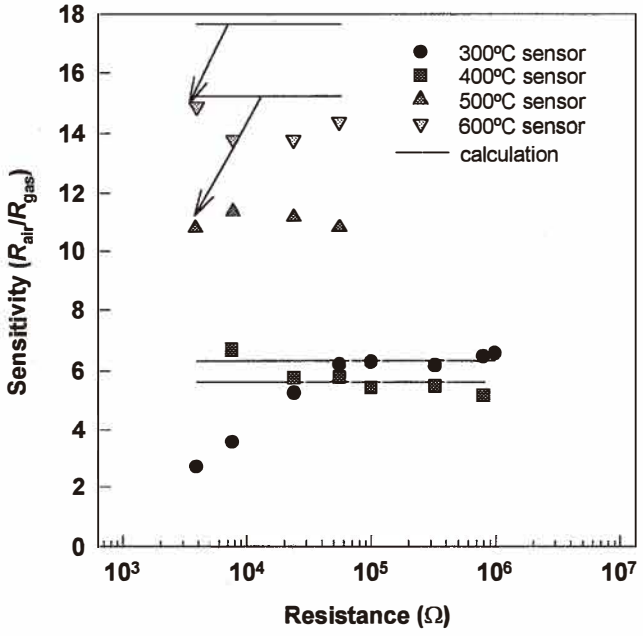

Fig. 7. Effect of series resistance on sensor resistance in (a) the conventional circuit and (b) the proposed circuit.

Table 1
C and α parameter of various sensors used in the experiments.

Sensor	*I-V* in air		*I-V* in gas	
	C	α	C	α
300°C SnO_2	1.5×10^{-7}	1.236	9.3×10^{-7}	1.248
400°C SnO_2	1.3×10^{-7}	1.784	1.0×10^{-6}	1.519
500°C SnO_2	9.9×10^{-7}	1.218	5.6×10^{-6}	1.833
600°C SnO_2	3.9×10^{-7}	1.780	2.3×10^{-6}	2.461

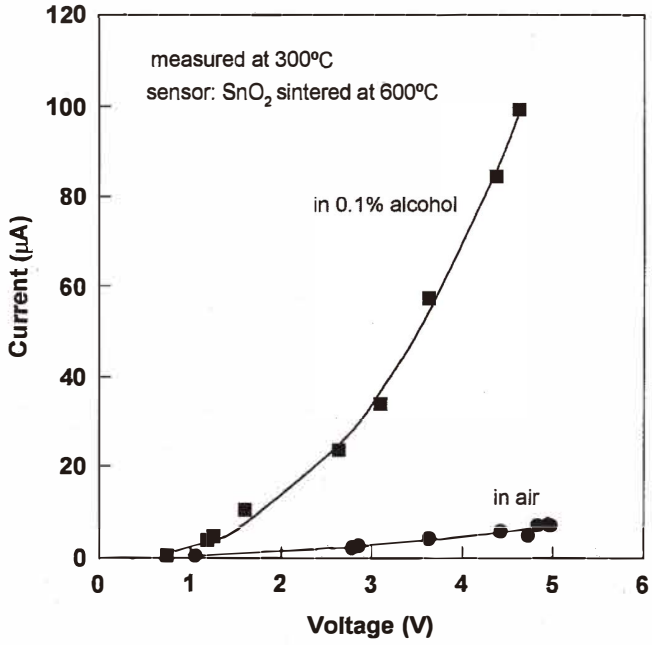

Fig. 8. Examples of *I-V* characteristics.

4.2 *Effect of external resistance on recovery time*

We also investigated the effect of the external resistance on recovery time, and the results are shown in Fig. 9. It was clarified that in the conventional circuit, all SnO_2 gas sensors exhibited the characteristic of recovery time being dependent on R. The values of recovery time increased with the values of R. In contrast, in the proposed circuit, no variation of recovery time with R could be observed (Fig. 9(b)). Moreover, the recovery time of the proposed circuit was faster than that of the conventional circuit.

(a)

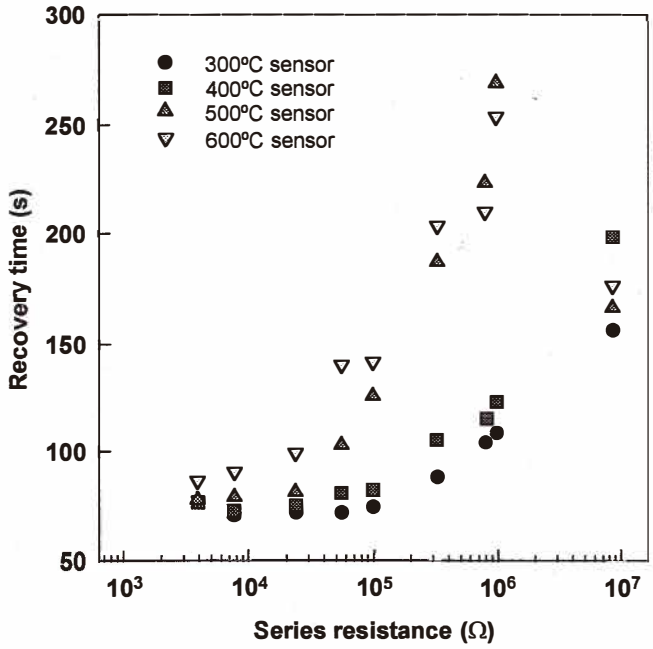

(b)

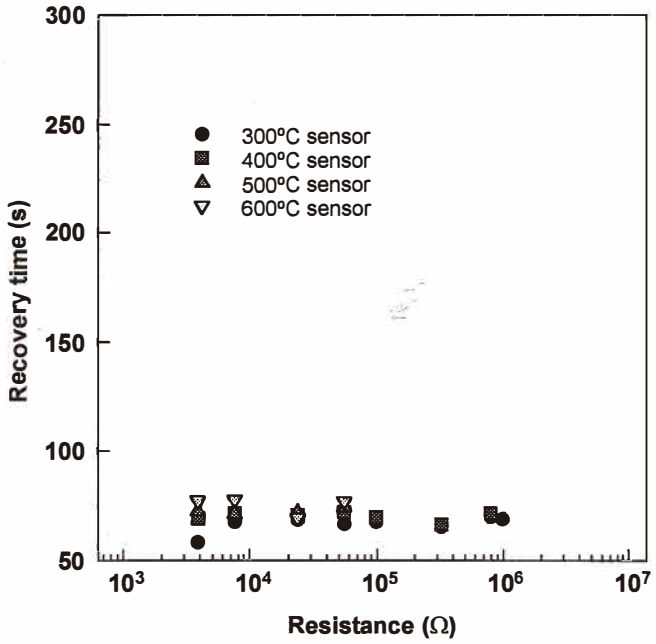

Fig. 9. Variation of recovery time with series resistance in (a) the conventional circuit and (b) the proposed circuit.

By considering the capacitance of the depletion layer at the grain boundary, it is reasonable to represent gas sensors by the electrical model in which resistance is connected in parallel with capacitance. Circuits including the dynamic model of gas sensors are shown in Fig. 10. Here, we elucidate the parameters contributing to sensor recovery time (T_r) as follows.

The conventional circuit: $T_r \propto \tau_1 + \tau_2 + \tau_3$
The proposed circuit: $T_r \propto \tau_1 + \tau_2$

Here, τ_1 is the time constant for the chemical reaction of oxygen readsorption on the SnO_2 surface after its reaction with alcohol. It is assumed that this constant does not depend on the electrical operating point of the gas sensor. τ_2 is the time constant of discharge through sensor resistance R_s, and junction capacitance C_s, and τ_3 are the time constant of discharge through external resistance R and junction capacitance, C_s, respectively.

It is clear that in the case of the conventional circuit, there was an additional term, τ_3, contributing to the recovery time. This term increases with the external resistance, which is consistent with the experimental results (Fig. 9(a)). In addition, by assuming an abrupt junction approximation, the total capacitance of the gas sensor can be given by

$$C_s \propto \frac{1}{\sqrt{V_o + V_s}}, \tag{10}$$

where V_o is the height of the potential barrier and V_s is the voltage at gas sensor terminals. In the case of the proposed circuit, where $V_s = V_{in}$, C_s is therefore constant. Consequently, the recovery time is constant and independent of the variation of the external resistance. For the conventional circuit, V_s depends on the external resistance, and the condition of V_s

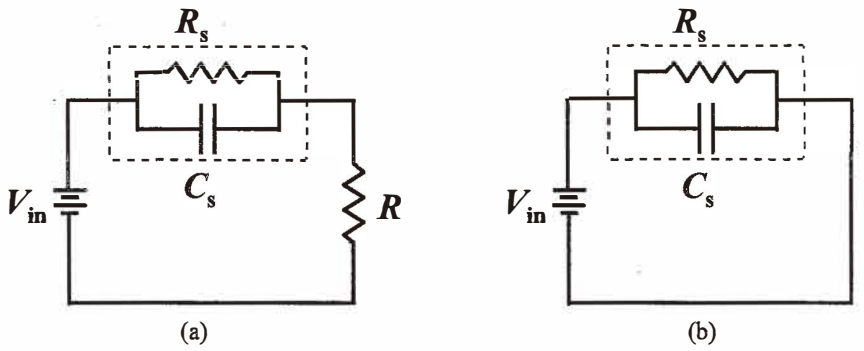

Fig. 10. Equivalent circuit of gas sensor for (a) the conventional circuit and (b) the proposed circuit.

$< V_{in}$ always holds, thus C_s of the conventional circuit is always greater than that of the proposed circuit.

5. Conclusions

The semiconductor gas sensors are now widely used in many applications because of their low cost and simplicity. However, so far, they have been neglected in basic research and development. Since there are numerous problems associated with their usage, a good understanding of their performance with respect to environmental conditions is essential. In this work, we considered the effect of the external resistance in the conventional circuit on gas sensitivity and recovery time. Theoretical analysis and experiments have been carried out using various SnO_2 sensors and a flow injection system. A new circuit, in which the sensor was biased at a fixed voltage, was proposed to solve these problems. The results showed that the new circuit provides a nearly constant sensitivity and faster recovery time independent of the external resistive component. We also believe that using this circuit, the gas sensitivities of various gas sensors from different sources can be compared quantitatively.

Acknowledgment

The authors would like to thank Kwanchai Anothainart for his help in preparing the SnO_2 powder and performing the BET analysis.

References

1 G. Heiland: Sensors and Actuators **2** (1982) 343.
2 S. R. Morrison: Sensors and Actuators **10** (1987) 283.
3 J. Millman and A. Grabel: Microelectronics (McGraw Hill, Singapore, 1988) p. 51.
4 T. Schubert, Jr. and E. Kim: Active and Non-linear Electronics (Wiley, New York, 1996) p. 62.
5 L. Hozer: Semiconductor Ceramics: Grain Boundary Effects (Ellis Horwood, London, 1994) p. 44.
6 T. Maekawa, J. Tamaki, N. Miura, N. Yamazoe and S. Matsushima: Sensors and Actuators B **9** (1992) 63.
7 J. S. Reed: Introduction to the Principle of Ceramic Processing (Wiley, Singapore, 1989) p. 47.
8 M. Sriyudthsak, L. Promsong and S. Panyakeow: Sensors and Actuators B **13 – 14** (1993) 139.
9 H. Ogawa, M. Nishikawa and A. Abe: J. Appl. Phys. **53** (1982) 4448.
10 C. Xu, J. Tamaki, N. Miura and N. Yamazoe: Sensors and Actuators B **3** (1991) 147.